Petroleum Science 20 (2023) 3428–3440

Contents lists available at ScienceDirect

Petroleum Science

journal homepage: www.keaipublishing.com/en/journals/petroleum-science

Original Paper

Quantitative characterization of tight gas sandstone reservoirs using seismic data via an integrated rock-physics-based framework

Zhi-Qi Guo*, Xiao-Ying Qin, Cai Liu

College of Geoexploration Science and Technology, Jilin University, Changchun, 130026, Jilin, China

ARTICLE INFO

Article history:
Received 21 February 2023
Received in revised form
24 May 2023
Accepted 4 September 2023
Available online 6 September 2023

Edited by Jie Hao and Meng-Jiao Zhou

Keywords:
Tight gas sandstone reservoirs
Quantitative reservoir characterization
Rock-physics-based framework
Microfracture porosity
Rock physics template

ABSTRACT

Seismic characterizing of tight gas sandstone (TGS) reservoirs is essential for identifying promising gas-bearing regions. However, exploring the petrophysical significance of seismic-inverted elastic properties is challenging due to the complex microstructures in TGSs. Meanwhile, interbedded structures of sandstone and mudstone intensify the difficulty in accurately extracting the crucial tight sandstone properties. An integrated rock-physics-based framework is proposed to estimate the reservoir quality of TGSs from seismic data. TGSs with complex pore structures are modeled using the double-porosity model, providing a practical tool to compute rock physics templates for reservoir parameter estimation. The V_P/V_S ratio is utilized to predict the cumulative thickness of the TGS reservoirs within the target range via the threshold value evaluated from wireline logs for lithology discrimination. This approach also facilitates better capturing the elastic properties of the TGSs for quantitative seismic interpretation. Total porosity is estimated from P-wave impedance using the correlation obtained based on wireline log analysis. After that, the three-dimensional rock-physics templates integrated with the estimated total porosity are constructed to interpret microfracture porosity and gas saturation from velocity ratio and bulk modulus. The integrated framework can optimally estimate the parameters dominating the reservoir quality. The results of the indicator proposed based on the obtained parameters are in good agreement with the gas productions and can be utilized to predict promising TGS reservoirs. Moreover, the results suggest that considering microfracture porosity allows a more accurate prediction of high-quality reservoirs, further validating the applicability of the proposed method in the studied region.

1. Introduction

As an unconventional reservoir, tight gas sandstone (TGS) reservoirs of the Ordos Basin, China, have produced large amounts of hydrocarbons (Zou et al., 2015; Du et al., 2018). As explorations and developments for TGS reservoirs move toward the margin regions of the Ordos Basin, where the region investigated in this paper is located, quantitative reservoir characterization through seismic methods is increasingly in demand (Li et al., 2016; Zheng et al., 2020). A successful seismic characterization should involve comprehensive estimations of reservoir properties, including, but not limited to, the cumulative thickness, gas saturation, and pore structures for TGS reservoirs (Yin et al., 2019; Guo et al., 2022a and b). In particular, TGSs in the region under exploration exhibit low porosity and extremely low permeability. Well-developed microfractures in TGSs are critical for fluid migration and accumulation and act as the primary determinants of high-quality reservoirs (Shu et al., 2021).

Although various prestack seismic inversion methodologies are capable of producing reliable estimates of elastic properties, the geological significance of the results obtained for TGS reservoirs should be explored via rock-physics-based approaches. Meanwhile, additional challenges arising from the interbedded structure of tight sandstone and mudstone should be suitably taken into account in the quantitative characterization of the target reservoir (Anees et al., 2019). Quantitative interpretation using the rock-physics templates (RPTs) offers a powerful tool for exploring the geological significance of seismic-inverted elastic properties (Ødegaard and Avseth, 2004). The RPTs could reveal complex correlations between elastic properties and reservoir parameters on specialized cross-plots, which can be utilized to transform the elastic properties obtained from seismic data into reservoir

* Corresponding author.
E-mail address: guozhiqi@jlu.edu.cn (Z.-Q. Guo).

https://doi.org/10.1016/j.petsci.2023.09.003

parameters. The RPTs-based approaches have been successfully exploited to characterize various hydrocarbon resources with particular reservoir properties. Some of these applications consist of lithology and fluid classification (Gupta et al., 2012) and cementation evaluation (Gial et al., 2021) for sandstones, fluid detection (Ba et al., 2013; Pang et al., 2019) and pore structure estimation (Pang et al., 2020) for carbonates, and oil saturation estimation (Carcione and Avseth, 2015) and sweet spot prediction (Zhao et al., 2016; Guo et al., 2022c) for shales.

In particular, various rock-physics-based approaches have been presented to characterize tight oil and gas reservoirs. A model-based workflow through a sophisticated inclusion model was proposed to quantitatively predict porosity and lithology in hybrid tight oil rocks to guide prestack elastic inversion for improved sweet spot prediction (Lu et al., 2019). A modeling method based on self-consistent approximation (SCA) and differential effective medium (DEM) theories has been implemented to build RPTs for the seismic prediction of brittleness in tight oil siltstones (Tan et al., 2020). The Biot-Rayleigh poroelasticity theory was utilized to compute templates for microcrack evaluation in TGSs (Ruan et al., 2021). In addition, the equivalent inclusion-average stress model was exploited to achieve elastic properties and construct RPTs to estimate the pore microstructure in TGSs (Cheng et al., 2021).

Despite successful approaches for predicting particular reservoir parameters via rock-physics-based methodologies, integrated frameworks for TGS reservoir characterization via RPTs have been rarely found in the existing literature. Moreover, rational modeling approaches are vital to performing rock physics modeling, estimating effective reservoir parameters, and constructing RPTs for tight rocks. As mentioned above, pore structure estimation is critical to assess the reservoir quality of TGSs in the region under investigation. So far, various methods for modeling elastic properties pertinent to pore structures in tight rocks have been explored by many scholars (David and Zimmerman, 2012; Zhang and Sun, 2018; Zhang et al., 2018). Complex pore structures in tight sandstones can be classified into spherical pores and microfractures (Smith et al., 2009; Ruiz and Cheng, 2010), which are commonly characterized by the double-porosity model based on the SCA or DEM theory. Meanwhile, other sophisticated double-porosity models (Sun et al., 2016; Ba et al., 2017) or multiple-porosity models (Zhang et al., 2020) are capable of describing more complex mechanics of poroelastic behaviors of tight rocks. The applicability of the double-porosity models was also confirmed by laboratory experiments (Wang, 2017; Yin et al., 2017).

In the present study, an integrated rock-physics-based framework is proposed for the quantitative seismic characterization of TGS reservoirs. For this purpose, the processes of the proposed framework are initially explained in some detail, followed by brief descriptions of the rock-physics models and the method for the evaluation of the pore structure via suitable models and wireline logs. In continuing, field data applications of the proposed framework are conducted for TGS reservoirs from the Ordos Basin. The evaluations pertinent to the pore structure are performed via wireline logs to confirm the validity of the double-porosity model. Quantitative seismic characterization on the basis of the wireline log analysis and constructed RPTs is adopted to capture the parameters affecting reservoir quality. Finally, the obtained results are effectively utilized to develop suitable indicators for identifying high-quality TGS reservoirs. The effectiveness of proposed indicators and the significance of microfractures are also assessed with the development status of gas-producing wells.

2. Methodology

2.1. Rock-physics-based framework for characterizing TGS reservoirs

The flowchart in Fig. 1 illustrates the proposed framework utilized for quantitatively characterizing TGS reservoirs based on seismic-derived elastic properties and wireline logs. The main processes of the integrated workflow are itemized in the following:

Step 1: Sufficient cumulative thickness TGS reservoirs (h) is the basis of gas enrichment. However, due to the low vertical resolutions of seismic data, distinguishing individual thin sandstone units interbedded with mudstones utilizing the reflection waveforms is challenging. Herein, we identify TGSs and assess their cumulative thickness in a target range via the V_P/V_S ratio from prestack seismic inversion. Particularly, the V_P/V_S threshold for discriminating tight sandstone and mudstone is determined from wireline log analysis. In the target range for seismic-inverted V_P/V_S ratio, the V_P/V_S values less than the threshold level are taken into account as the indication of TGS reservoirs. The counted time samples with low V_P/V_S values in the target range are suitably correlated to h by the calibration with log interpretation results in existing wells. In this sense, a greater number of samples with low V_P/V_S values suggest a larger h for the target range. The actual data applications for h estimation of the target TGS reservoirs are provided in section 3.3.1, where the h-map for the target reservoir is illustrated as the output.
Step 2: The total porosity (φ) of TGS reservoirs is essential for gas accumulation and can be estimated from the P-wave impedance (I_P) in the studied region. Section 3.2.2 of this paper demonstrates that there exists an evident correlation between φ and I_P for TGS reservoirs using wireline log analysis. Accordingly, an appropriate linear regression between φ and I_P is established from the wireline logs and then applied to elastic inversion results to realize φ estimation using seismic data. In field data applications, the I_P values for TGS reservoirs in the target range are extracted employing the V_P/V_S threshold determined in step 1. After calibration using wireline logs, this step produces the φ-map for the target reservoir. The estimation of φ from I_P is fairly straightforward; however, it would be a crucial procedure for constructing three-dimensional (3D) RPTs, as explained in the next step.
Step 3: Quantitative seismic interpretation based on the 3D-RPTs is the core of the integrated framework presented in Fig. 1. First, an appropriate rock-physics model (RPM) is necessary to compute RPTs. In section 2.2, the feasibility of the double-porosity model is methodically evaluated. The primary advantage of the employed model is the exploitation of microfracture porosity (φ_f) to describe microstructures of pore spaces. Microfractures are essential for TGS reservoirs, providing migration pathways for fluid flow to form gas reservoirs with sufficient gas saturation (S_g).

In this step, the 3D-RPTs of (φ_f, S_g) for varying φ are constructed on the cross-plots of (K, V_P/V_S), where K denotes the bulk modulus of rock. In this sense, the three dimensions include the reservoir parameters φ, φ_f, and S_g. It is worth mentioning that the templates are computed using K instead of the commonly used I_P, where the superiority of K for characterizing TGS reservoirs was discussed by Yang et al. (2017) and Guo et al. (2022c). After calibration using

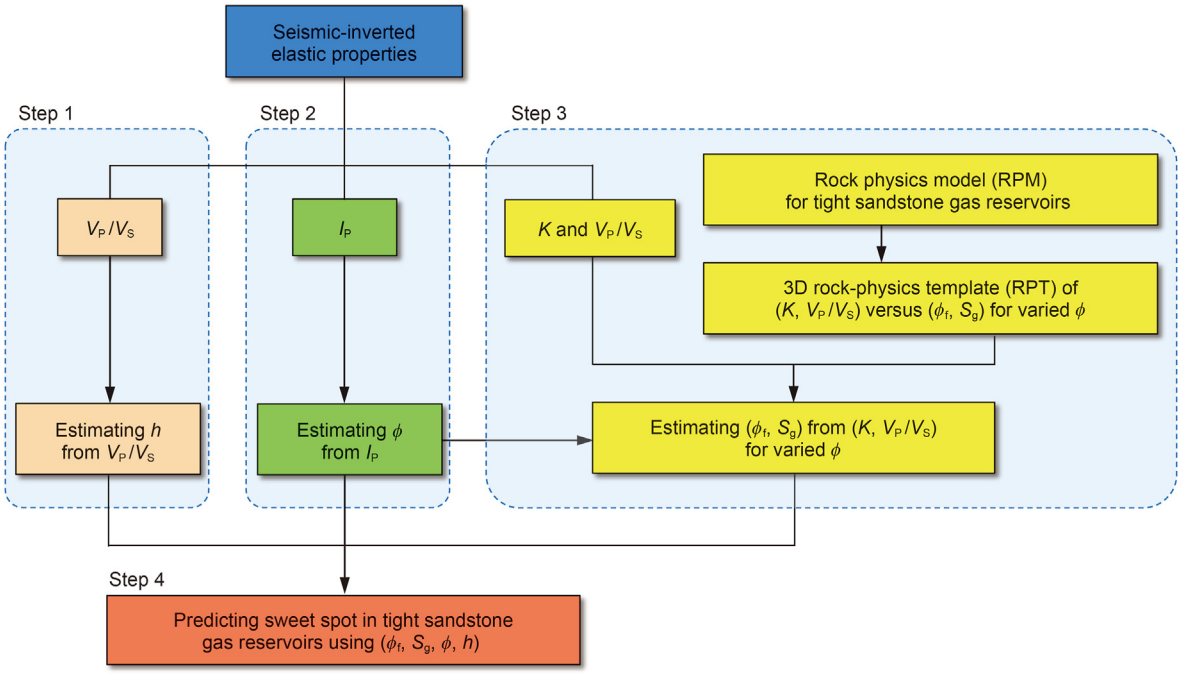

Fig. 1. An integrated rock-physics-based framework for quantitative seismic characterization of TGS reservoirs.

wireline logs, the constructed 3D-RPTs are utilized to interpret reservoir parameters (φ_f, S_g) from seismic-obtained elastic properties (K, V_P/V_S) for varying φ estimated at step 2. The values of K and V_P/V_S for the TGS reservoirs in the target range are obtained using the V_P/V_S threshold presented in step 1. The construction of 3D-RPTs and the corresponding applications to field data are presented in section 3.2.3. The outputs include the maps of φ_f and S_g for the target TGS reservoirs.

Step 4: The rational results of h, φ, φ_f, and S_g allow reliable evaluation of the TGS reservoirs utilizing the obtained parameters that primarily affect reservoir quality. In this step, a novel indicator is appropriately introduced that comprehensively takes the estimated reservoir parameters into account. The effectiveness of the proposed indicator and the significance of microfractures for reservoir quality are explored by the calibration with the production status of gas wells.

2.2. Rock-physics models for TGS reservoirs

In the framework presented in Fig. 1, establishing appropriate RPM for TGSs is essential for computing 3D-RPTs. As shown by the thin-section images of the TGS reservoirs from the studied region (see Fig. 2), the complex pore space in the solid matrix can be classified into two primary types, namely, spherical pores (stiff pores) and microfractures (soft pores) according to Ruiz and Cheng (2010). Therefore, the double-porosity model is implemented to describe the TGSs with these pore microstructures.

For comparison, schematic representations of two models for TGSs have been illustrated in Fig. 3, which includes the single-porosity model (see Fig. 3a) and the double-porosity model (see Fig. 3b). The aspect ratio (α) is employed in the single-porosity model to estimate pore geometry with a porosity of φ. In the double-porosity model, the total pore space (φ) consists of spherical or stiff pores (φ_p) and microfractures (φ_f).

In the work of Guo and Li (2015), the SCA method was proved more applicable than the SCA-Gassmann method for modeling tight rock such as shale. The reason was attributed to the fact that the Gassmann theory assumes sufficient hydraulic communication and pore-pressure equilibrium, which may not apply to tight rock. Our numerical test results (not displayed in this paper) following the work of Guo and Li (2015) also suggest that the SCA method is more applicable than the SCA-Gassmann method for modeling TGS in the study area.

The modeling workflows for the two models are demonstrated in Fig. 4a and 4b, respectively. The moduli of the solid matrix are modeled by employing the Hashin-Shtrikman bounds (HSB) method (Hashin and Shtrikman, 1963). The equivalent bulk (K) and shear moduli (μ) of the mineral matrix can be obtained as follows:

$$K^{HS+} = \Lambda(\mu_{max}), K^{HS-} = \Lambda(\mu_{min}) \tag{1}$$

$$\mu^{HS+} = \Gamma(\zeta(K_{max}, \mu_{max})), \mu^{HS-} = \Gamma(\zeta(K_{min}, \mu_{min})) \tag{2}$$

and

$$\Lambda(z) = \langle \frac{1}{K(r) + \frac{4}{3}z} \rangle - \frac{4}{3}z \quad \Gamma(z) = \langle \frac{1}{\mu(r) + z} \rangle^{-1} - z \quad \zeta(K, \mu) = \frac{\mu}{6}\left(\frac{9K + 8\mu}{K + 2\mu}\right) \tag{3}$$

where the superscripts HS+ and HS- in order are the upper and lower bounds, K_{max} and K_{min} correspond to the maximum and minimum bulk moduli of consisting minerals of the solid matrix, respectively. Further, μ_{max} and μ_{max} represent the maximum and minimum shear moduli of the minerals, $K(r)$ and $\mu(r)$ are the bulk and shear moduli of the r-th minerals in the mineral matrix, and the symbol $\langle \cdot \rangle$ stands for the weighted average of the quantities.

The SCA theory (Berryman, 1980) is employed to describe the influence of pore geometry through a single aspect ratio (see Fig. 4a). Meanwhile, the SCA theory is utilized to model the pore

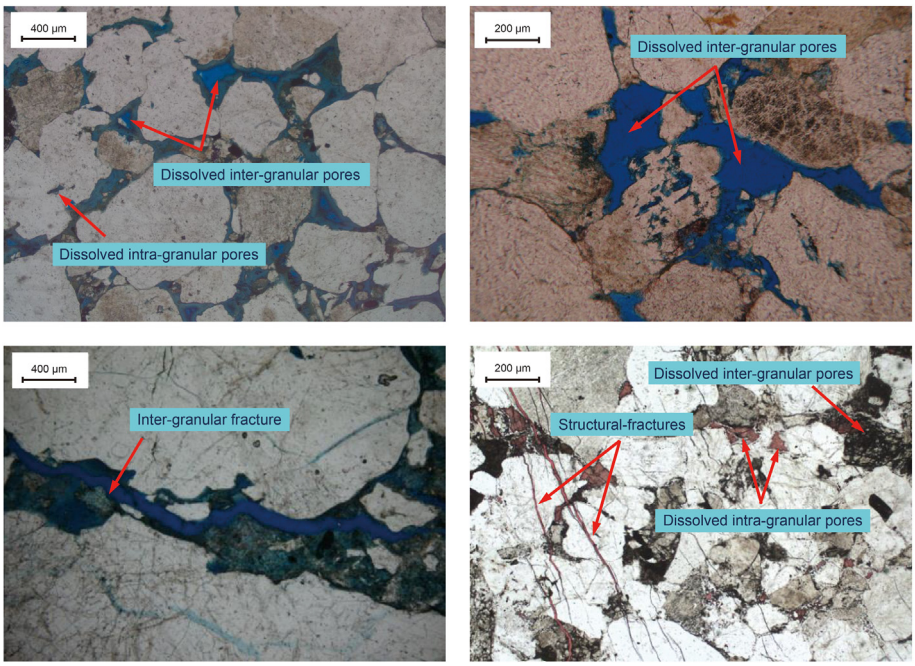

Fig. 2. Thin-section images of TGSs from the studied region in the Ordos Basin.

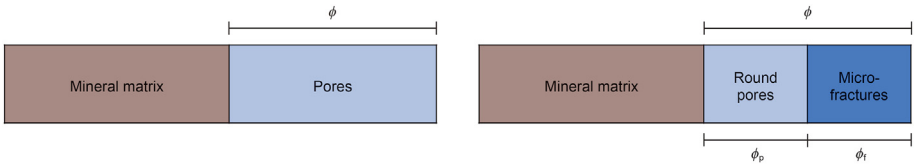

Fig. 3. Schematic representations of two modes for TGSs: (a) single-porosity model and (b) double-porosity model.

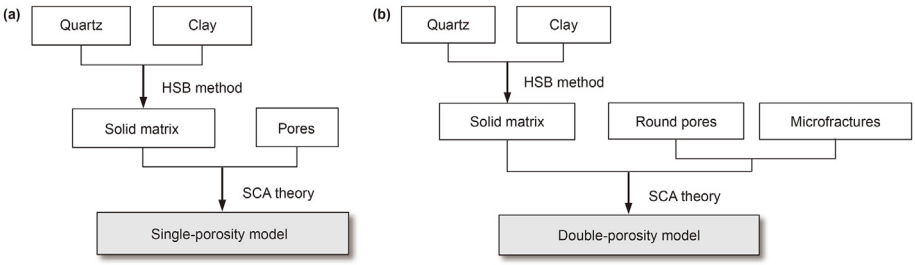

Fig. 4. Rock-physics modeling workflows of (a) single-porosity model and (b) double-porosity model.

spaces consisting of spherical pores and microfractures with varying volume fractions (see Fig. 4b). Since the SCA theory is essentially established based on the high-frequency assumption, it is suitable for modeling pores and microfractures as inclusions in tight rocks with low matrix permeability. The effective bulk modulus (K_{SC}^{*}) and shear modulus (μ_{SC}^{*}) of a medium composed of multiple phases are calculated by the SCA theory in the following forms:

$$\sum_{j=1}^{n} f_j (K_j - K_{SC}^{*}) P^{*j} = 0 \tag{4}$$

$$\sum_{j=1}^{n} f_j \left(\mu_j - \mu_{SC}^{*}\right) Q^{*j} = 0 \tag{5}$$

where f_j is the volume fraction of the j-th constituent, K_j and μ_j represent the corresponding bulk and shear modulus of the j-th constituent, geometric factors of the j-th constituent in the host material are denoted by P^{*j} and Q^{*j}, and n is the number of constituents.

For the fluids distributed in pore spaces with poor connectivity, Jia (2018) suggested that the formula of Domenico (1977) is more applicable for computing the fluid bulk modulus K_f of TGS:

$$K_f = S_w K_w + S_g K_g \tag{6}$$

where S_w and S_g in order denote the water and gas saturations, and K_w and K_g represent the bulk moduli of water and gas, respectively.

The fluid mixture density is obtained by:

$$\rho_f = S_w\rho_w + S_g\rho_g \quad (7)$$

where ρ_w and ρ_g signify the water and gas density, respectively.

2.3. Pore structure evaluation for TGS reservoirs using wireline logs

Based on the models presented in section 2.2, pore structures can be quantified using the parameter α in the single-porosity model (Figs. 3a and 4a) and φ_f in the double-porosity model (Figs. 3b and 4b). This section deals with an approach to assess the effectiveness of the two models and the corresponding pore parameters. The main criterion is to compare the prediction accuracy of the shear wave velocity (V_S) using wireline logs for the two models. As a general rule, higher V_S prediction accuracy indicates better applicability of the model and corresponding pore parameters for the TGS reservoirs. Fig. 5 illustrates V_S prediction and pore parameter estimation flowcharts based on the single-porosity model (left) and the double-porosity model (right) using wireline logs.

Specifically, the pore parameters α and φ_f are treated as the fitting parameters in the procedure of V_S prediction. The inputs of the prediction model of V_S include volume fractions of minerals, porosity, and fluid properties, which can be obtained from wireline logs. The proposed approach seeks particular values of α and φ_f that minimize the discrepancy between the P-wave velocity (V_P) measured in a borehole (V_P-measured) and that calculated via the model (V_P-calculated) at each logging interval. To this end, the grid-searching approach can be effectively implemented to achieve this process for predetermined α and φ_f values. The obtained α and φ_f could be considered the crucial parameters exploited for the pore structure evaluation. In addition, the simultaneously obtained $V_S(\alpha)$ and $V_S(\varphi_f)$ for the estimated α and φ_f are treated as the V_S prediction results. As mentioned above, the errors in V_S prediction are used to assess the applicability of the employed models and the corresponding pore parameters for TGS reservoirs in the region under exploration.

3. Results

3.1. Datasets

The datasets are taken from the TGS reservoirs of the Ordos Basin, China (see Fig. 6). The studied region in this paper is positioned near the edge of the eastern border of the basin. The target TGS reservoirs have formed several large gas fields with vast amounts of natural gas. The map of the two-way travel time (see Fig. 7) and the interpreted horizon on the seismic profile (see Fig. 8) for the target reservoir reveal that the tectonic relief of the local region is relatively flat. The TGS reservoirs with well-developed pores and microfractures are essential for gas accumulation.

Wireline logs of three wells, namely, A, B, and C, are available in the region of interest (see Fig. 7), allowing rock-physic analysis, prediction of the pore structure, and calibration of the constructed 3D-RPTs (see Fig. 1). The elastic properties are achieved utilizing prestack seismic inversion. Fig. 9 illustrates V_P/V_S, I_P, and K profiles derived from the elastic inversion results. For a better understanding of the correlation between wireline logs and seismic responses, detailed results of the seismic-well tie for the target TGS in Well B can be found in the work of Guo et al. (2022). Using the method presented in the framework of Fig. 1, the elastic properties of the TGS reservoirs in the target range are extracted using the V_P/V_S threshold (estimated as 1.85 via the wireline logs) and then averaged to produce the maps of V_P/V_S, I_P, and K, as demonstrated in Fig. 10. The properties given in Fig. 10 will be exploited as inputs for estimating reservoir parameters (h, φ, φ_f, and S_g) based on the approach displayed in Fig. 1.

3.2. Pore structure estimation and V_S prediction based on RPMs using wireline logs

We conduct pore structure estimation and V_S prediction on the basis of the approaches presented in Fig. 5 and wireline logs from the three wells with locations displayed in Fig. 7. The composition properties used for modeling are given in Table 1. Aspect ratios of spherical pores and microfractures are assumed to be 1 and 0.01, according to Ruiz and Cheng (2010). The computed results based on

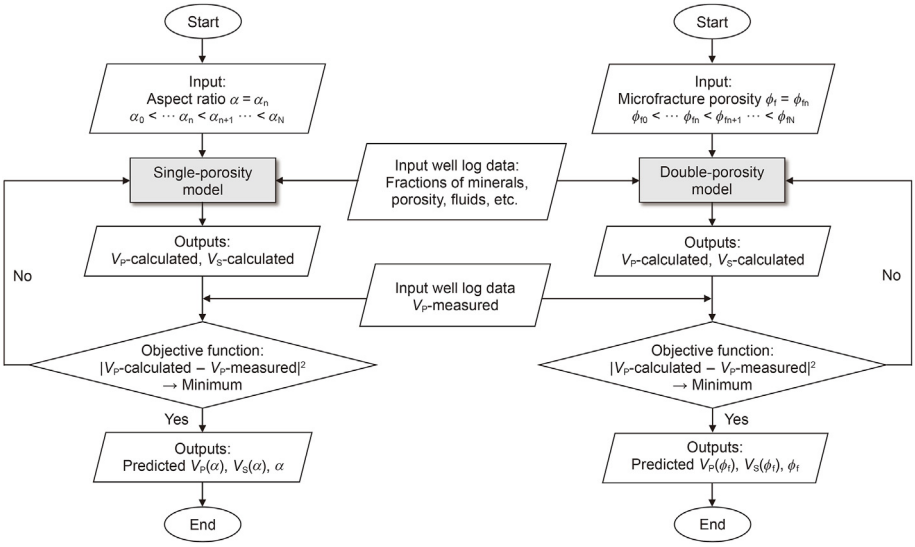

Fig. 5. Flowcharts proposed for predictions of V_S and pore parameters of the TGS reservoirs based on the single-porosity and the double-porosity models.

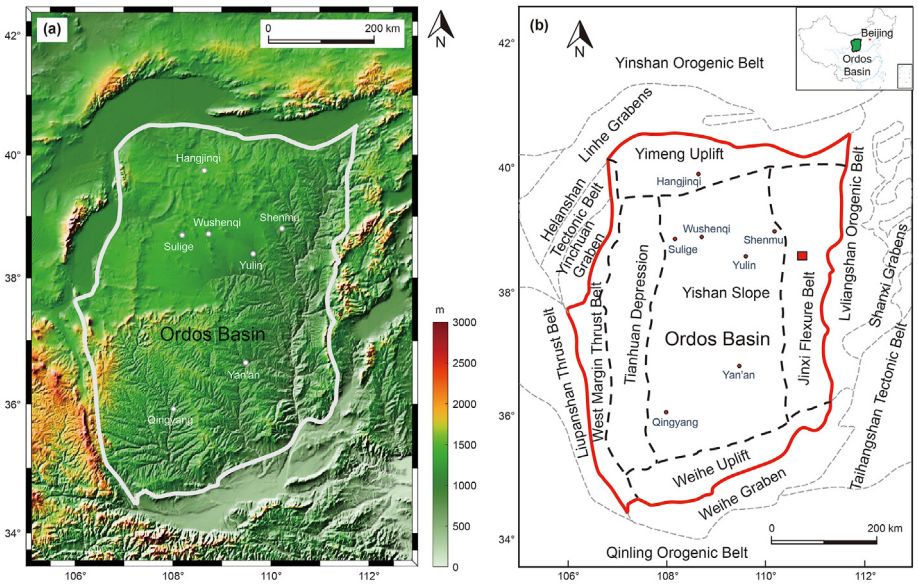

Fig. 6. The Ordos Basin: (a) Contemporary relief map, (b) regional geological map. (note: red rectangles indicate the studied region in this paper).

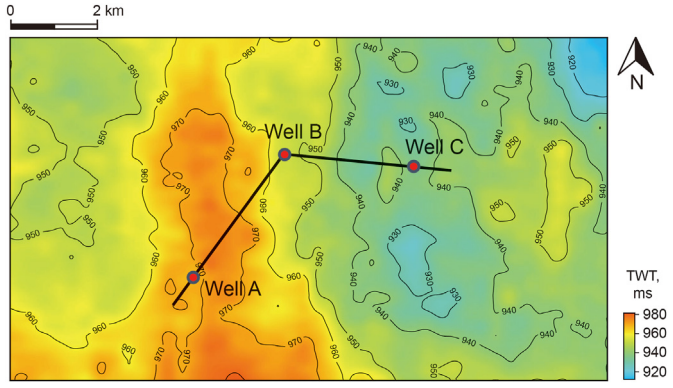

Fig. 7. Map of two-wave travel time for the target TGS reservoirs (note: red dots signify the locations of wells A, B, and C; black lines present seismic lines across the three wells).

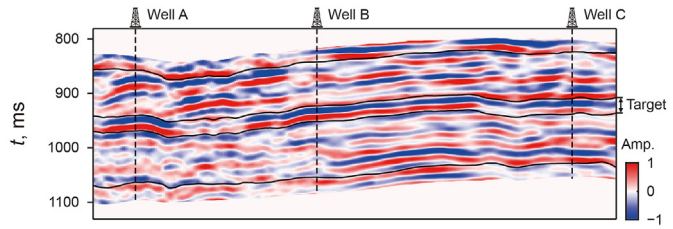

Fig. 8. The post-stack profile with seismic line presented in Fig. 7.

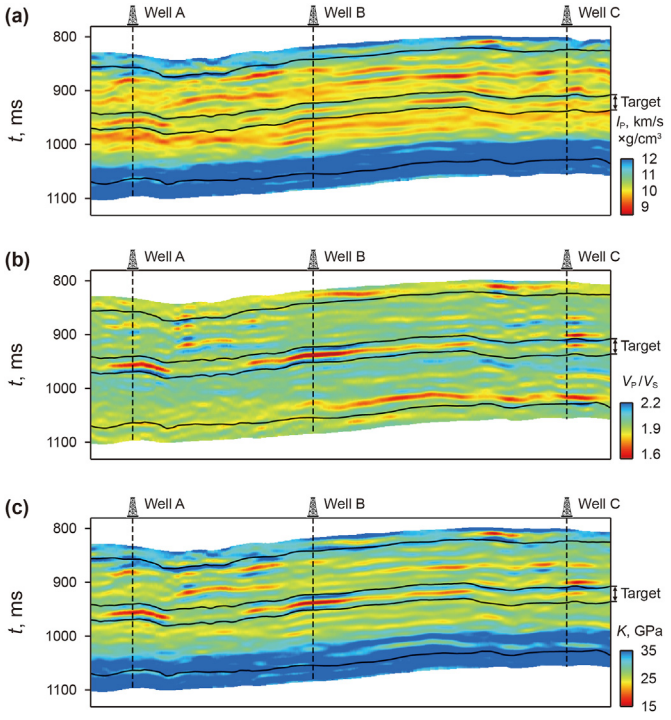

Fig. 9. Various profiles of the seismic line presented in Fig. 7: (a) I_P, (b) V_P/V_S, and (c) K.

the single-porosity and double-porosity models for the three considered wells in order are illustrated in Figs. 11 and 12. As can be seen, the computed V_P satisfactorily fit with the measured values by adjusting the α in the single-porosity model (see Fig. 11) and φ_f in the double-porosity model (see Fig. 12).

For the three wells, the correlation coefficients between the predicted V_S values and those measured are 0.88, 0.90, and 0.89 based on α (see Fig. 11), and 0.93, 0.95, and 0.93 based on φ_f (see Fig. 12). The achieved results reveal the double-porosity model is capable of providing a more accurate V_S prediction. This fact suggests that this model and the corresponding pore parameter (φ_f) should be more applicable to the target reservoirs in the studied region. Further, the estimated φ_f in Fig. 12 can be effectively employed to calibrate the constructed 3D-RPTs in the following sections.

3.3. Quantitative seismic characterization of TGS reservoirs

3.3.1. Estimating h for TGS reservoirs using V_P/V_S

Based on the method presented in step 1 in section 2.1 (see Fig. 1), the values of h for TGS reservoirs in the target range is evaluated. The estimated results are illustrated in Fig. 13, which has

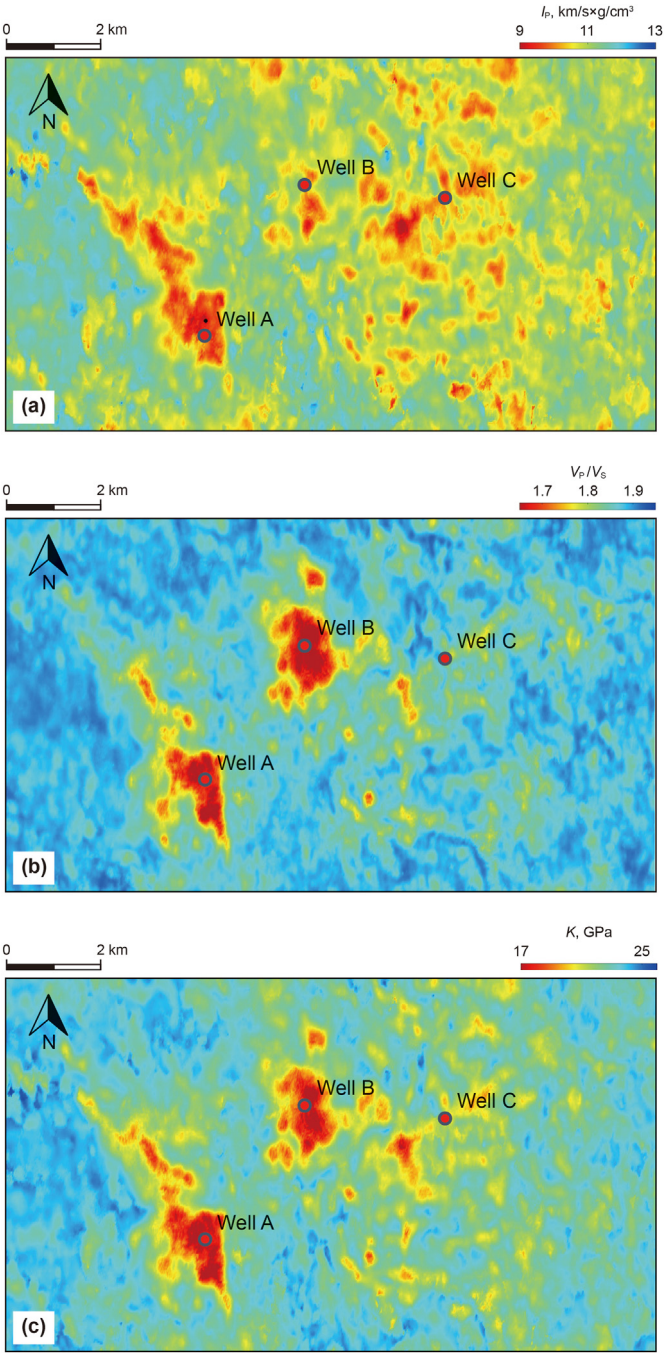

Fig. 10. Various maps of the TGS reservoirs corresponding to Fig. 9: (a) I_P, (b) V_P/V_S, and (c) K.

Table 1
Composition properties used in the present paper (Mavko et al., 2009).

	Quartz	Clay	Gas	Water
K, GPa	36.60	21.00	0.012	2.25
μ, GPa	45.00	7.00	–	–
P, g/cm^3	2.65	2.60	0.078	1.04

been calibrated with the logging interpretation results using wireline logs from Fig. 12. The values of h are comparable in Well A and Well B and are higher than that in Well C, which is consistent with the interpretation of the wireline logs presented in Fig. 12.

3.3.2. *Predicting φ for TGS reservoirs using I_P*

Based on the wireline logs from the three wells in Fig. 12, the complementary analysis shows that I_P and φ of TGS reservoirs apparently exhibit linear negative correlation (see Fig. 14). The established linear regression in Fig. 14 is then employed to transform seismic-inverted I_P into φ. It can be anticipated that the distribution of φ (see Fig. 15) is similar to I_P (see Fig. 10a) owing to the evident linear correlations between the two variables. As illustrated in Fig. 15, the values of φ are comparable in the three wells, which is consistent with the achieved results revealed from the wireline logs (see Fig. 12). However, the high-porosity TGS reservoirs cover a wider region, exhibiting a delta sedimentary lithofacies adjacent to Well A.

According to the geological understanding of the study area, TGSs usually have a low porosity and those with a porosity of less than 0.1 can form effective reservoirs in the Ordos Basin. However, some sandstones may have a porosity of up to 0.15 and form premium reservoirs, which is a special case as shown in the local area illustrated in Fig. 15.

3.3.3. *Quantitative interpretation of φ_f and S_g based on 3D-RPTs*

The 3D-RPTs proposed in the third step of section 2.1 (see Fig. 1) could be implemented as a critical technique for predicting reservoir parameters in TGS reservoirs. This subsection demonstrates the construction of the 3D-RPTs and the corresponding applications in the quantitative prediction of φ_f and S_g using seismic data. For this purpose, the double-porosity model, whose effectiveness for characterizing TGS reservoirs has been validated in section 3.2, is employed to compute the 3D-RPTs.

Fig. 16 illustrates the computed 3D-RPTs of (φ_f, S_g) on the cross-plots of (V_P/V_S, K) for varying φ, where the reservoir parameters have the ranges of 0–0.05 for φ_f, 0–1.0 for S_g, and 0.02–0.20 for φ. In real data applications, these ranges should cover possible variations of the reservoir parameters, and the size of intervals should be small enough to ensure rational accuracy in parameter estimations. The composition properties utilized for modeling are given in Table 1. To this end, the average volume fractions of quartz and clay for TGS are set as 0.95 and 0.05 according to wireline log interpretation in Fig. 12. Moreover, the templates are color-coded in terms of E/λ, representing the brittleness index (BI) proposed by Chen et al. (2014). The constructed 3D-RPTs provide insights into complex correlations among the elastic properties (V_P/V_S, K), the reservoir properties (φ_f, S_g, φ), and the brittleness index. The 3D-RPTs in Fig. 16 can be exploited for the quantitative interpretation of seismic data after appropriate calibration with wireline logs.

As demonstrated in Fig. 17, the wireline logs of TGS reservoirs from the three wells (see Fig. 12) are superimposed on the RPT. The presented template corresponds to the case of $\varphi = 0.13$ (i.e., the average porosity of the TGS reservoirs in the three wells). The relative discrepancies in the φ_f and S_g values, as indicated by the template for the three wells, are consistent with the corresponding relationships displayed in Fig. 12. In the calibration of RPTs using wireline logs, the primary challenge comes from the reservoir heterogeneity, which is represented by the scatting distribution of data points.

Fig. 18 illustrates the 3D-RPTs in Fig. 16, along the axis of porosity for convenience, where the seismic data for the target TGS reservoirs from Fig. 10 are superimposed on the templates. As demonstrated in Fig. 15, the values of φ have been estimated from I_P (see Fig. 10a) for each data point in Fig. 18. The spatial correspondence of various factors in Figs. 10 and 15 indicate that each pair of V_P/V_S and K in Fig. 18 corresponds to a specific level of φ. Therefore, the data points in Fig. 18 can be color-coded by φ, as highlighted in Fig. 19. Most importantly, the plotted results in Fig. 19 indicate the necessity of estimating φ before conducting quantitative interpretation

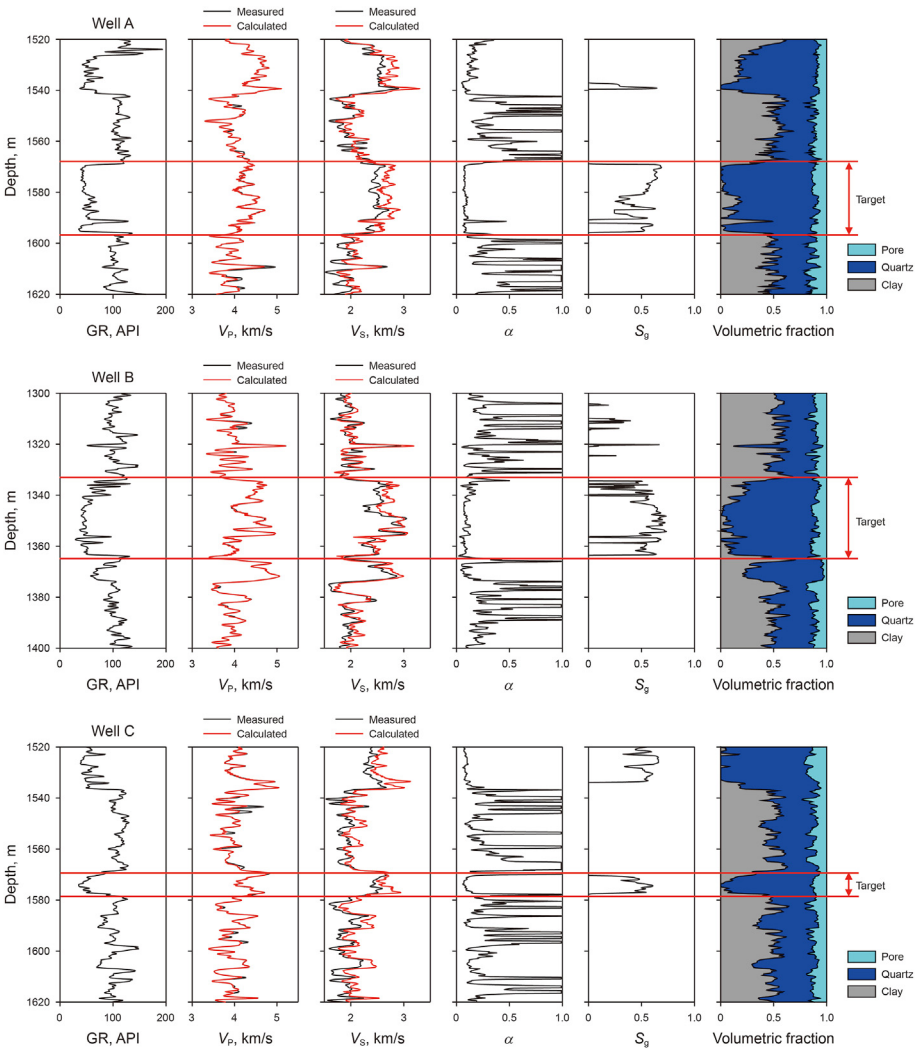

Fig. 11. Wireline logs, including *GR*, V_P, V_S, α, S_g, and volume fractions of minerals for different wells. (note: red lines indicate the target TGS reservoirs. Velocity curves in black correspond to the measured values, and velocity curves in red are associated with those calculated results on the basis of the single-porosity model).

via RPTs in Fig. 18. Subsequently, according to the given step 3 in Fig. 1, appropriate templates are chosen for each data point in Fig. 18. To this end, the depicted results in Figs. 18 and 19 are used to interpret reservoir parameters (φ_f, S_g) from seismic data (V_P/V_S, K) for each particular φ. The estimated results of φ_f and S_g for the tight sandstone gas reservoirs are demonstrated in Fig. 20.

3.3.4. Evaluation of BI in TGS

The brittleness of TGS determines its ability to be fracked by hydraulic fracturing, which affects the ultimate gas production of reservoirs. As suggested by Chen et al. (2014), BI determined by E/λ can provide an appropriate evaluation of rock brittleness. In Fig. 21, we illustrated the BI which can be derived from elastic properties in Fig. 10. The result indicates that TGS at Well A and Well B exhibites higher BI than Well C. In the following section, BI will be incorporated into the factors proposed for the comprehensive characterization of TGS.

3.3.5. Identification of high-quality TGS reservoirs using estimated reservoir parameters

Based on the integrated rock-physics-based framework presented in Fig. 1, we have derived reservoir parameters (see Figs. 13, 15, 20 and 21) that control the reservoir quality of TGSs. Subsequently, the estimated reservoir parameters are utilized for comprehensively characterizing TGS reservoirs. Certainly, the high-quality TGS reservoirs could be appropriately characterized by large cumulative thickness (h), high gas saturation (S_g), sufficient porosity (φ), well-developed microfractures (φ_f), and high BI. To this end, we define the factors associated with these reservoir factors to evaluate reservoir quality for TGSs. Specifically, two normalized factors, F_1=*Normalized*($h \times S_g \times$ BI $\times \varphi$) and F_2=*Normalized*($h \times S_g \times$ BI $\times \varphi \times \varphi_f$), are proposed for comparison. The main goal is to explore the effect of φ_f since microfractures are considered to be substantial for the effective development of TGS reservoirs in the studied region.

Fig. 22a and 22b illustrate maps of F_1 and F_2, respectively, where the primary discrepancy is associated with the anomaly values of F_1 and F_2 adjacent to Well B. For quantitative comparison, the normalized values of F_1 and F_2 for the TGS reservoirs at the three wellbore locations are extracted and illustrated in Fig. 23a. The results reveal that the F_2 value at Well B is comparable with that at Well C, and both values are lower than the corresponding value at Well A. In comparison, the F_1 value at Well B is comparable to that of Well A, and both of these values are higher than the corresponding values at Well C.

To examine the effectiveness of the results provided in Fig. 23a, the gas production status for the three wells is illustrated, as presented in Fig. 23b. The predicted results suggest that Wells B and C

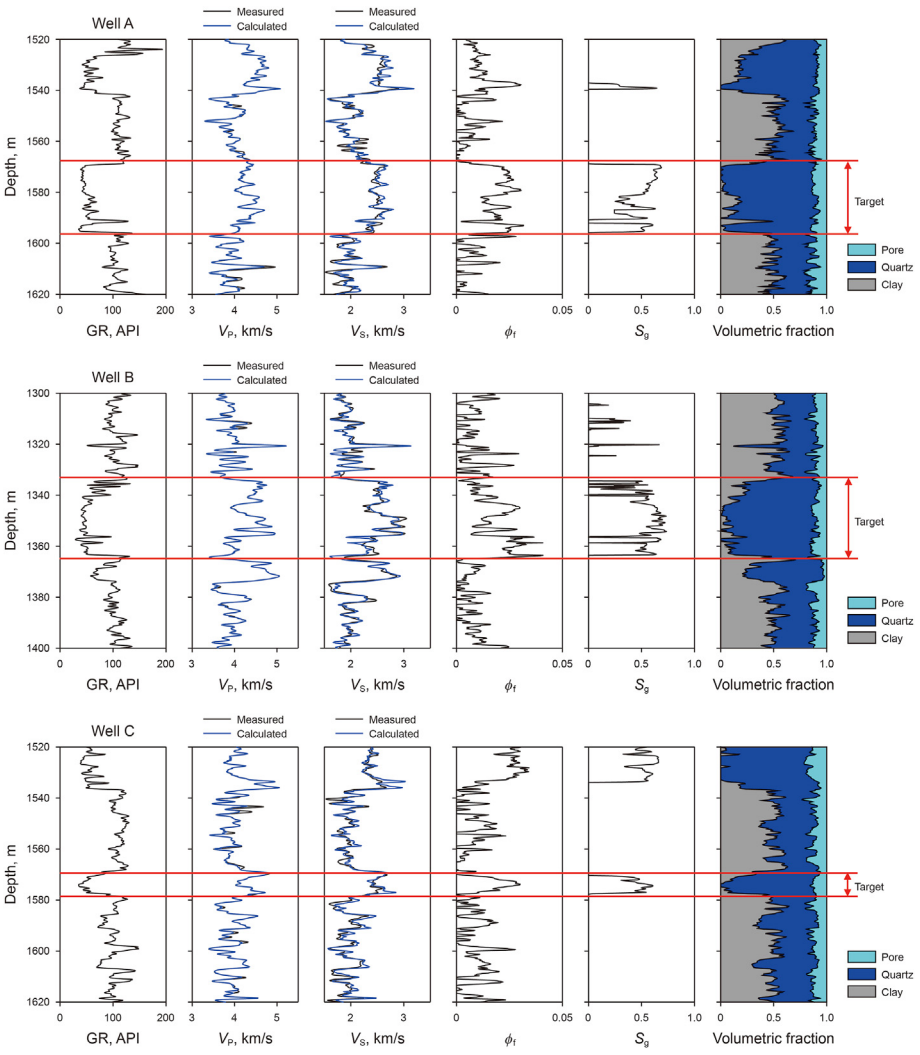

Fig. 12. Wireline logs, including *GR*, V_P, V_S, φ_f, S_g, and volume fractions of minerals for different wells. (Notes: red lines indicate the target TGS reservoirs. Velocity curves in black correspond to the measured values, and velocity curves in blue are associated with those calculated results on the basis of the double-porosity model).

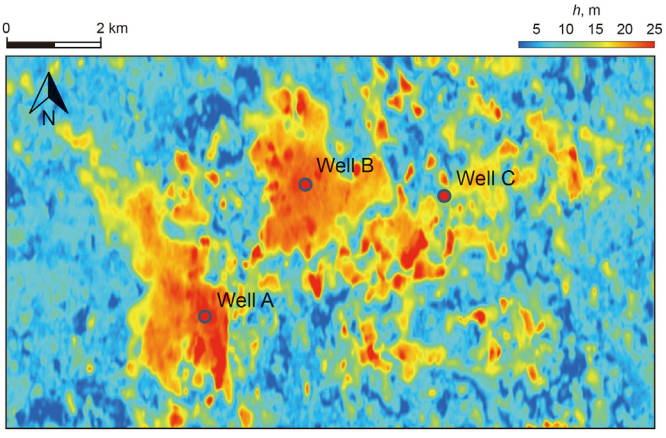

Fig. 13. Map of the estimated *h* for the target TGS reservoirs.

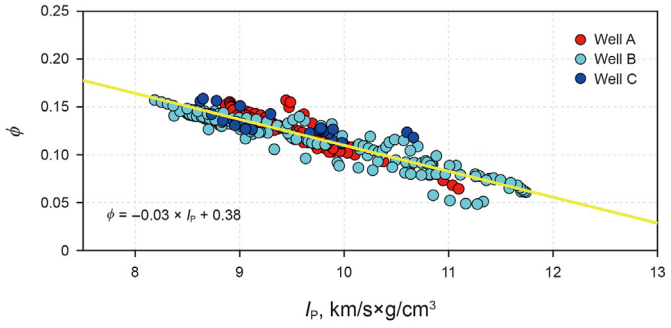

Fig. 14. Cross-plot of φ and I_P for the target TGS reservoirs from the three wells. (note: the yellow line represents the linear fitting relationship of the data).

produce a similar amount of gas, which is lower than that of Well A. It indicates that the gas production (see Fig. 23b) exhibits an apparent correlation with the factor F_2 (see Fig. 23a), confirming the effectiveness of F_2 in the identification of high-quality TGS reservoirs. Most importantly, the above comparison between F_1 and F_2 reveals the significance of microfractures (φ_f) for predicting gas production in TGS reservoirs.

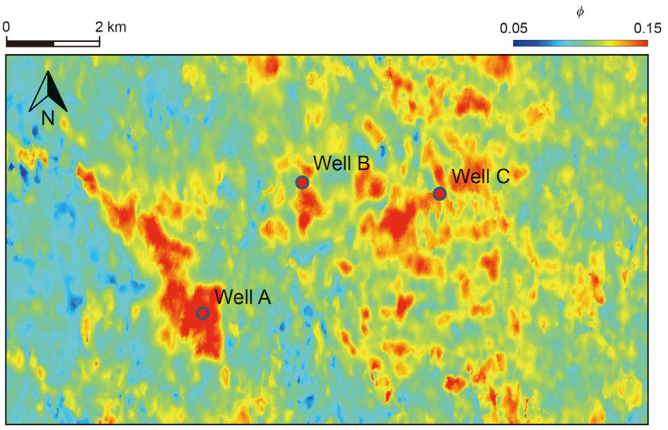

Fig. 15. Map of φ of the target TGS reservoirs estimated from I_P based on the linear regression relationship displayed in Fig. 14.

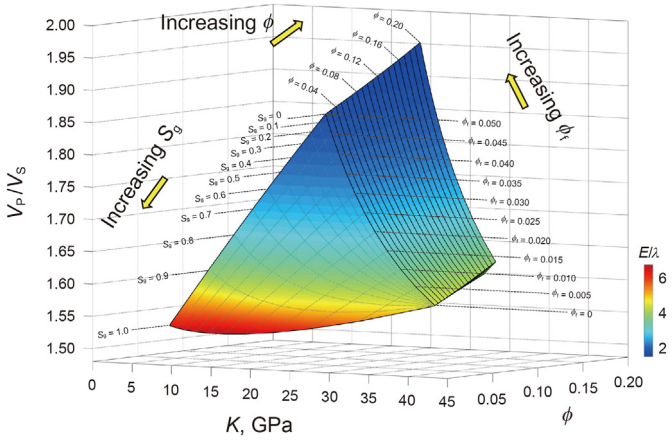

Fig. 16. The correlations between the elastic properties (V_P/V_S, K) and the reservoir properties (φ_f, S_g, φ) based on the 3D-RPTs. (note: the templates are color-coded by E/λ, which represents the brittleness index).

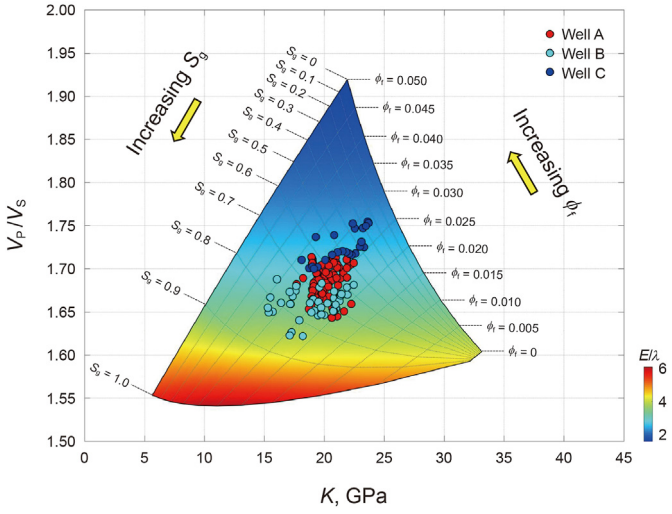

Fig. 17. Calibration of the RPT using the wireline logs from Fig. 12. (note: the template is color-coded by E/λ, which represents the brittleness index).

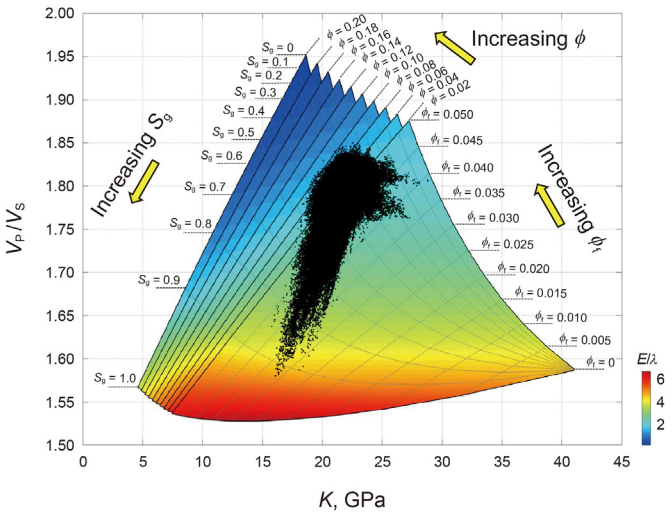

Fig. 18. Two-dimensional display of 3D-RPTs for quantitative interpretation of reservoir parameters (φ_f, S_g) using seismic-derived elastic properties (V_P/V_S, K). (note: the templates are color-coded by E/λ, which specifies the brittleness index. The seismic data have been superimposed on the templates).

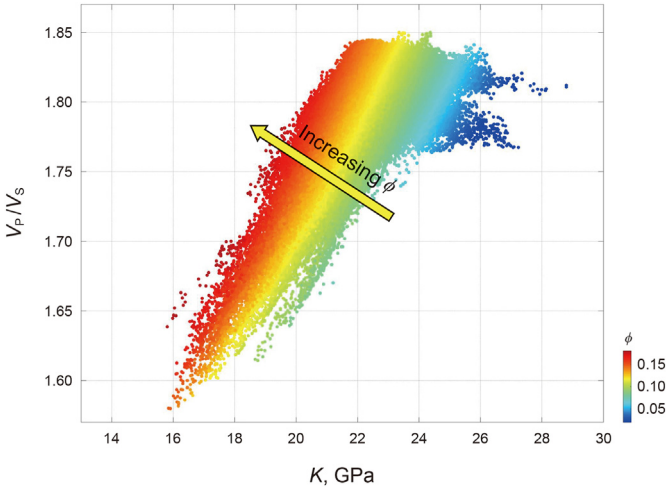

Fig. 19. The V_P/V_S and K cross-plot superimposed with the seismic-derived data for the TGS reservoirs from Fig. 10. (note: the data points are color-coded by φ estimated in Fig. 15, such that the arrow indicates the trend of increasing φ).

4. Discussion

4.1. Advantages of the proposed framework for characterizing TGS reservoirs

We have proposed an integrated framework for quantitatively characterizing TGS reservoirs via a rock-physics-based framework (see Fig. 1). First, the approach of estimating the cumulative thickness of TGS reservoirs based on the V_P/V_S threshold is suitable for thin-layered sandstones and mudstones, where the traditional interpretation methodology vis seismic waveforms could not be applicable for such an interbedded structure. Moreover, it provides a practical method to extract seismic-derived elastic properties for TGS reservoirs in the target ranges, which are essential for rock

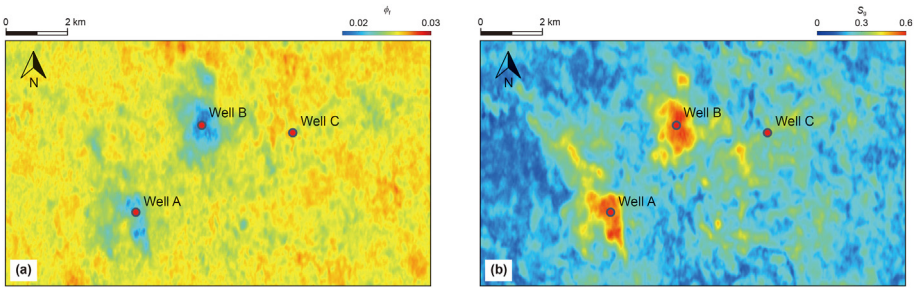

Fig. 20. Maps of the predicted parameters for the TGS reservoirs: (a) φ_f, (b) S_g.

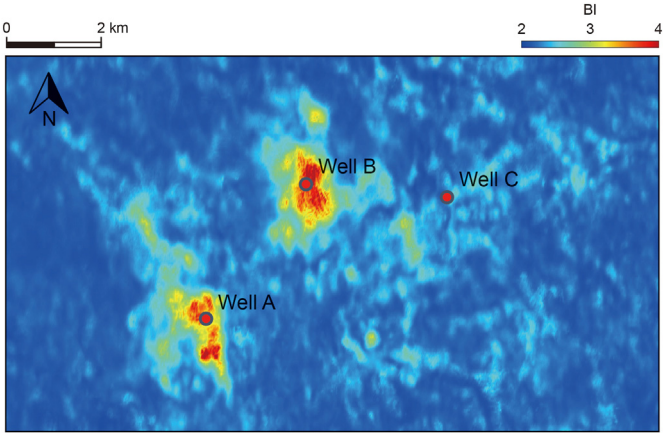

Fig. 21. Map of BI for the TGS reservoirs.

physics analysis and quantitative interpretation in the subsequent processes. In addition, the obtained linear correlation between I_P and φ is critical for optimizing the reservoir characterization scheme, making it feasible to estimate (φ_f, S_g) based on (K, V_P/V_S) for varying φ via the constructed 3D-RPTs (see Figs. 18 and 19). This optimal framework guarantees robust and reliable interpretation of seismic data, particularly applicable to the case of the multi-parameter prediction displayed in Fig. 1. The estimated reservoir parameters (see Figs. 13, 15 and 20) capture the dominant factors influencing reservoir quality and allow comprehensive characterization of TGS reservoirs. The factor determined on the basis of the estimated reservoir parameters (see Fig. 21b) exhibits an obvious correlation with gas production (see Fig. 22). This suggests the proposed factor is an effective indicator for identifying promising TGS reservoirs. Further, comparisons between the two factors, as shown in Fig. 21, suggest that microfractures are crucial in affecting gas production. This issue provides insights for a better understanding of tight gas sandstones in the studied region.

4.2. Appropriate modeling methods for TGSs

Rational rock-physics models and appropriate reservoir parameters are essential for describing microstructures of TGS reservoirs and computing templates for reservoir characterization. The practicability of the employed double-porosity model and the corresponding parameter φ_f for pore structure description has been validated by the results of V_S prediction (see Fig. 12). Meanwhile,

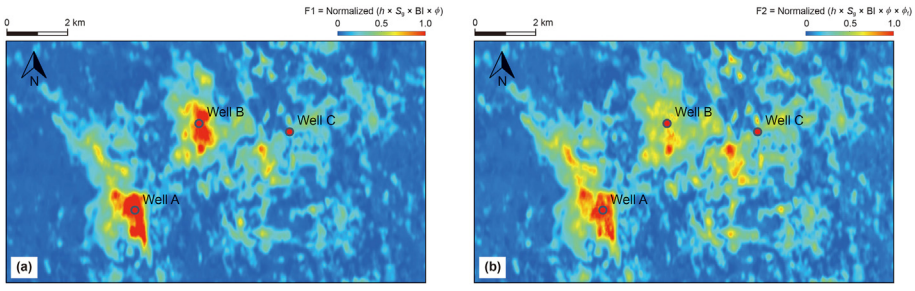

Fig. 22. Maps of two factors for comprehensive characterization of the TGS reservoirs: (a) F_1=*Normalized*($h \times S_g \times$ BI $\times \varphi$) and (b) F_2= *Normalized*($h \times S_g \times$ BI $\times \varphi \times \varphi_f$).

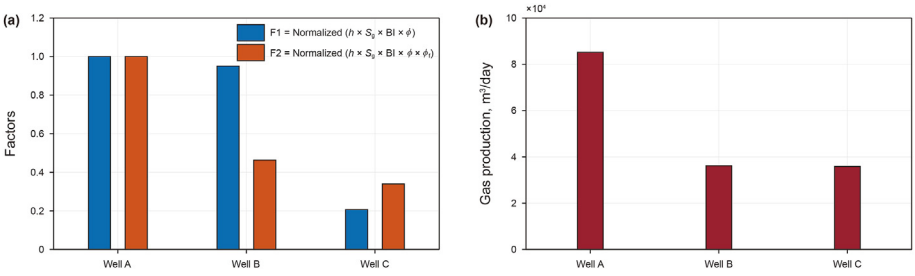

Fig. 23. The target TGS reservoirs in the three wells: (a) values of F_1 and F_2, (b) gas production status.

the Pore structures quantified by φ_f have been proven critical to gas production.

Nevertheless, based on the improved understanding of the TGS microstructures, other sophisticated methods could be included for modeling elastic and inelastic properties associated with heterogeneous fabric and patchy saturation in TGSs (Sun et al., 2016; Ba et al., 2017). Seismic attenuation can also be estimated to provide valuable information for improved characterization of tight gas sandstones (Picotti et al., 2018; Pang et al., 2020). In addition, this paper is aimed to explore pores and microfractures with randomly-distributed orientations in TGSs, which are described with isotropic models. In fact, vertical tectonic fractures in the TGS reservoirs are not taken into account in the present model and could be scrutinized using azimuthal seismic anisotropy (Guo et al., 2022; Zhang et al., 2022).

4.3. Limitations of RPTs for quantitative seismic interpretation

The primary limitation of RPTs for quantitatively interpreting seismic data is that they are site-specific. The RPMs applicable to one region might not be straightforwardly extended to other regions. It is chiefly attributed to the variations in microstructures for rocks from various regions that make developing universal models impossible. An improved understanding of TGS characteristics based on geological and petrophysics properties can also provide insights for constructing rational models and proposing effective parameters in reservoir characterization.

Another inherent limitation is that the construction of RPTs tends to be target-oriented, meaning that estimation of reservoir parameters via the templates may be suitable for a specific target layer rather than formations with wide depth ranges. It is the primary reason that restricts the proposed method from producing horizontal maps of various reservoir parameters for the target TGS reservoir.

Finally, the essence of quantitative seismic interpretation involves transforming elastic properties into reservoir parameters via RPTs. To this end, appropriate procedures should be designed based on rock physics analysis to lessen the resulting uncertainties in multiple parameter estimation using elastic properties. As mentioned, the obtained correlation allows rational predicting φ from I_P first, followed by interpreting (φ_f, S_g) from (K, V_P/V_S) for varying φ using 3D-RPTs. This integrated scheme ensures the robustness of multi-parameter estimation using RPTs and could provide helpful references for optimizing the quantitative characterization process in other hydrocarbon resources.

5. Conclusions

This study has been conducted to explore the quantitative seismic characterization of TGS reservoirs using an integrated rock-physics-based framework. The proposed methodology is capable of optimally capturing the primary reservoir parameters that determine reservoir quality, including cumulative thickness, total porosity, microfracture porosity, and gas saturation for TGS reservoirs. The cumulative thickness and total porosity of TGS reservoirs are appropriately predicted using rock-physics analysis and wireline logs. These processes result in the integrated estimation of microfracture porosity and gas saturation, which are interpreted from V_P/V_S ratio and bulk modulus for varying total porosity via the constructed 3D-RPTs. The predicted shear wave velocity has proven that the double-porosity model is capable of effectively characterizing the microstructures of TGS reservoirs and providing a practical tool for computing rock-physics templates.

The indicator proposed based on the estimated reservoir parameters is consistent with the gas production; hence, it could effectively identify promising TGS reservoirs. Meanwhile, analysis indicates that the predicted microfracture porosity exhibits a critical influence on gas production, indicating the necessity of the pore structure evaluation as well as the applicability of the proposed scheme for reservoir characterization in the region under investigation. Finally, the approach developed in the current work could inspire the development of potentially efficient rock-physics-based approaches for identifying other hydrocarbon reservoirs.

Declaration of competing interest

The authors declare that they have no known competing financial interests or personal relationships that could have appeared to influence the work reported in this paper.

Acknowledgments

This work was supported by the National Natural Science Foundation of China (Grant numbers 42274160 and 42074153).

References

Anees, A., Shi, W.Z., Ashraf, U., et al., 2019. Channel identification using 3D seismic attributes and well logging in lower Shihezi Formation of Hangjinqi area, northern Ordos Basin, China. J. Appl. Geophys. 163, 139–150. https://doi.org/10.1016/j.jappgeo.2019.02.015.

Ba, J., Cao, H., Carcione, J.M., et al., 2013. Multiscale rock-physics templates for gas detection in carbonate reservoirs. J. Appl. Geophys. 93, 77–82. https://doi.org/10.1016/j.jappgeo.2013.03.011.

Ba, J., Xu, W.H., Fu, L.Y., et al., 2017. Rock anelasticity due to patchy saturation and fabric heterogeneity: a double double-porosity model of wave propagation. J. Geophys. Res. Solid Earth 122, 1949–1976. https://doi.org/10.1002/2016jb013882.

Berryman, J.G., 1980. Long-wavelength propagation in composite elastic media II. Ellipsoidal inclusions. J. Acoust. Soc. Am. 68, 1820–1831. https://doi.org/10.1121/1.385172.

Carcione, J.M., Avseth, P., 2015. Rock-physics templates for clay-rich source rocks. Geophysics 80, D481–D500. https://doi.org/10.1190/geo2014-0510.1.

Chen, J.J., Zhang, G.Z., Chen, H.Z., et al., 2014. The construction of shale rock physics effective model and prediction of rock brittleness. SEG Technical Program Expanded Abstracts 2014, 2861–2865. doi:10.1190/segam2014-0716.1.

Cheng, W., Ba, J., Carcione, J.M., et al., 2021. Estimation of the pore microstructure of tight-gas sandstone reservoirs with seismic data. Front. Earth Sci. 9, 646372. https://doi.org/10.3389/feart.2021.646372.

David, E.C., Zimmerman, R.W., 2012. Pore structure model for elastic wave velocities in fluid-saturated sandstones. J. Geophys. Res. Solid Earth 117, B07210. https://doi.org/10.1029/2012JB009195.

Domenico, S.N., 1977. Elastic properties of unconsolidated porous sand reservoirs. Geophysics 42, 1339–1368. https://doi.org/10.1190/1.1440797.

Du, S.H., Pang, S., Shi, Y.M., 2018. A new and more precise experiment method for characterizing the mineralogical heterogeneity of unconventional hydrocarbon reservoirs. Fuel 232, 666–671. https://doi.org/10.1016/j.fuel.2018.06.012.

Guo, Z.Q., Li, X.Y., 2015. Rock physics model-based prediction of shear wave velocity in the Barnett Shale formation. J. Geophys. Eng. 12, 527–534. https://doi.org/10.1088/1742-2132/12/3/527.

Guo, Z.Q., Lv, X.Y., Liu, C., et al., 2022a. Shale gas characterisation for hydrocarbon accumulation and brittleness by integrating a rock-physics-based framework with effective reservoir parameters. J. Nat. Gas Sci. Eng. 100, 104498. https://doi.org/10.1016/j.jngse.2022.104498.

Guo, Z.Q., Nie, N.F., Liu, C., 2022b. Fracture characterization based on improved seismic amplitude variation with azimuth inversion in tight gas sandstones, Ordos Basin, China. Mar. Petrol. Geol. 146, 105941. https://doi.org/10.1016/j.marpetgeo.2022.105941.

Guo, Z.Q., Zhao, D.Y., Liu, C., 2022c. Gas prediction using an improved seismic dispersion attribute inversion for tight sandstone gas reservoirs in the Ordos Basin, China. J. Nat. Gas Sci. Eng. 101, 104499. https://doi.org/10.1016/j.jngse.2022.104499.

Guo, Z.Q., Zhao, D.Y., Liu, C., 2022d. A new seismic inversion scheme using fluid dispersion attribute for direct gas identification in tight sandstone reservoirs. Rem. Sens. (21), 5326.

Gupta, S.D., Chatterjee, R., Farooqui, M.Y., 2012. Rock physics template (RPT) analysis of well logs and seismic data for lithology and fluid classification in Cambay Basin. Int. J. Earth Sci. 101, 1407–1426. https://doi.org/10.1007/s00531-011-0736-1.

Hashin, Z., Shtrikman, S., 1963. A variational approach to the theory of the elastic behavior of multiphase materials. J. Mech. Phys. Solid. 11, 127–140. https://doi.org/10.1016/0022-5096(63)90060-7.

Jia, L.Y., 2018. Study on seismic fluid discrimination technology of tight gas

reservoir. Northwest University, Shanxi Xian (in Chinese).
Li, Y., Tang, D.Z., Wu, P., et al., 2016. Continuous unconventional natural gas accumulations of Carboniferous-Permian coal-bearing strata in the Linxing area, northeastern Ordos basin, China. J. Nat. Gas Sci. Eng. 36, 314–327. https://doi.org/10.1016/j.jngse.2016.10.037.
Lu, M.H., Cao, H., Sun, W.T., et al., 2019. Quantitative prediction of seismic rock physics of hybrid tight oil reservoirs of the Permian Lucaogou Formation, Junggar Basin, Northwest China. J. Asian Earth Sci. 178, 216–223. https://doi.org/10.1016/j.jseaes.2018.08.014.
Ødegaard, E., Avseth, P., 2004. Well log and seismic data analysis using rock physics templates. First Break 22, 37–43. https://doi.org/10.3997/1365-2397.2004017.
Pang, M.Q., Ba, J., Carcione, J.M., et al., 2019. Estimation of porosity and fluid saturation in carbonates from rock-physics templates based on seismic Q. Geophysics 84, M25–M36. https://doi.org/10.1190/geo2019-0031.1.
Pang, M.Q., Ba, J., Fu, L.Y., et al., 2020. Estimation of microfracture porosity in deep carbonate reservoirs based on 3D rock-physics templates. Interpretation 8, 1–41. https://doi.org/10.1190/INT-2019-0258.1.
Picotti, S., Carcione, J.M., Ba, J., 2018. Rock-physics templates based on seismic Q. Geophysics 84, 1–36. https://doi.org/10.1190/geo2018-0017.1.
Ruan, C.T., Ba, J., Carcione, J.M., et al., 2021. Microcrack porosity estimation based on rock physics templates: a case study in Sichuan basin, China. Energies 14, 7225. https://doi.org/10.3390/en14217225.
Ruiz, F., Cheng, A., 2010. A rock physics model for tight gas sand. Lead. Edge 29, 1484–1489. https://doi.org/10.1190/1.3525364.
Shu, Y., Sang, S.X., Lin, Y.X., et al., 2021. The influence of magmatic-hydrothermal activities on porosity and permeability of sandstone reservoirs in the Linxing area, Ordos Basin, Northern China. J. Asian Earth Sci. 213, 104741. https://doi.org/10.1016/j.jseaes.2021.104741.
Smith, T.M., Sayers, C.M., Sondergeld, C.H., 2009. Rock properties in low-porosity/low-permeability sandstones. Lead. Edge 28, 48–59. https://doi.org/10.1190/1.3064146.
Sun, W.T., Ba, J., Carcione, J.M., 2016. Theory of wave propagation in partially saturated double-porosity rocks: a triple-layer patchy model. Geophys. J. Int. 205, 22–37. https://doi.org/10.1093/gji/ggv551.
Tan, W.H., Ba, J., Müller, T., et al., 2020. Rock physics model of tight oil siltstone for seismic prediction of brittleness. Geophys. Prospect. 68, 1554–1574. https://doi.org/10.1111/1365-2478.12938.
Wang, D.X., 2017. A study on the rock physics model of gas reservoir in tight sandstone. Chin. J. Phys. 60, 64–83. https://doi.org/10.1002/cjg2.30028.
Yang, H., Wang, D., Zhang, M., et al., 2017. Seismic prediction method of pore fluid in tight gas reservoirs, Ordos Basin, NW China. Petrol. Explor. Dev. 44 (4), 544–551. https://doi.org/10.1016/S1876-3804(17)30063-0.
Yin, H.J., Zhao, J.G., Tand, G.Y., et al., 2017. Pressure and fluid effect on frequency-dependent elastic moduli in fully saturated tight sandstone. J. Geophys. Res. Solid Earth 122, 8925–8942. https://doi.org/10.1002/2017jb014244.
Yin, S., Han, C., Wu, Z.H., et al., 2019. Developmental characteristics, influencing factors and prediction of fractures for a tight gas sandstone in a gentle structural area of the Ordos Basin, China. J. Nat. Gas Sci. Eng. 72, 103032. https://doi.org/10.1016/j.jngse.2019.103032.
Zhang, J.J., Yin, X.Y., Zhang, G.Z., 2020. Rock physics modelling of porous rocks with multiple pore types a multiple-porosity variable critical porosity model. Geophys. Prospect. 68, 955–967. https://doi.org/10.1111/1365-2478.12898.
Zhang, T.T., Sun, Y.F., 2018. Two-parameter prestack seismic inversion of porosity and pore-structure parameter of fractured carbonate reservoirs Part 1 — methods. Interpretation 6, SM1–SM8. https://doi.org/10.1190/INT-2017-0219.1.
Zhang, T.T., Zhang, R.F., Tian, J.Z., et al., 2018. Two-parameter prestack seismic inversion of porosity and pore-structure parameter of fractured carbonate reservoirs Part 2 — applications. Interpretation 6, SM9–SM17. https://doi.org/10.1190/INT-2018-0019.1.
Zhang, Y.Y., Jiang, S., He, Z.L., et al., 2022. Characteristics of heterogeneous diagenesis and modification to physical properties of Upper Paleozoic tight gas reservoir in eastern Ordos Basin. J. Petrol. Sci. Eng. 208, 109243. https://doi.org/10.1016/j.petrol.2021.109243.
Zhao, L.X., Qin, X., Han, D.H., et al., 2016. Rock-physics modeling for the elastic properties of organic shale at different maturity stages. Geophysics 81, 527–541. https://doi.org/10.1190/geo2015-0713.1.
Zheng, D.Y., Pang, X.Q., Jiang, F.J., et al., 2020. Characteristics and controlling factors of tight sandstone gas reservoirs in the Upper Paleozoic strata of Linxing area in the Ordos Basin, China. J. Nat. Gas Sci. Eng. 75, 103135. https://doi.org/10.1016/j.jngse.2019.103135.
Zou, C.N., Zhai, G.M., Zhang, G.Y., et al., 2015. Formation, distribution, potential and prediction of global conventional and unconventional hydrocarbon resources. Petrol. Explor. Dev. 42, 14–28. https://doi.org/10.1016/S1876-3804(15)60002-7.